Downloaded from rsta.royalsocietypublishing.org

PHILOSOPHICAL TRANSACTIONS OF THE ROYAL SOCIETY A
MATHEMATICAL, PHYSICAL & ENGINEERING SCIENCES

Preliminary Observations of the Magellanic Clouds with the Ultraviolet Sky Survey Telescope

R. G. Evans, K. Nandy and R. Wilson

Phil. Trans. R. Soc. Lond. A 1975 **279**, 473-477
doi: 10.1098/rsta.1975.0083

Email alerting service Receive free email alerts when new articles cite this article - sign up in the box at the top right-hand corner of the article or click **here**

To subscribe to *Phil. Trans. R. Soc. Lond. A* go to: **http://rsta.royalsocietypublishing.org/subscriptions**

This journal is © 1975 The Royal Society

Downloaded from rsta.royalsocietypublishing.org

Phil. Trans. R. Soc. Lond. A. **279**, 473–477 (1975) [473]
Printed in Great Britain

Preliminary observations of the Magellanic Clouds with the ultraviolet sky survey telescope

By R. G. Evans
Appleton Laboratory, Culham Laboratory, Abingdon, Oxfordshire

K. Nandy
Royal Observatory Edinburgh

and R. Wilson
University College London, Gower Street, London W.C.1

[Plates 17 and 18]

Observations of the Magellanic Clouds have been made with the ultraviolet sky-survey telescope (S2-68) on board the E.S.R.O. satellite TD-1A. From the data so far reduced, the ultraviolet surface brightness has been derived for four wavelength bands centred near 1550, 1950, 2350 and 2740 Å. Ultraviolet maps of the Large Magellanic Cloud are presented and the flux distributions in each cloud are compared with that expected from a galactic luminosity function.

The S2-68 experiment

The observations to be described in this paper were performed in 1972 by the sky-survey experiment S2-68 in the E.S.R.O. satellite TD-1A. The S2-68 experiment (Boksenberg *et al.* 1973) carries out a controlled scan of the sky and obtains ultraviolet spectra of point sources, reaching about 9th visual magnitude for early-type stars. The instrument consists of a 27.5 cm diameter reflecting telescope which sequentially feeds a grating spectrograph and photometer which employ a total of four photomultiplier detectors. The orbital motion of the telescope causes the stellar image to move across the entrance slot of the spectrograph and the spectrum, from 1350 to 2550 Å is scanned across three fixed exit slits. The image then moves into the slot of the photometer whose response has a central wavelength of 2740 Å and a bandwidth of about 300 Å. When the telescope views extended objects in the spectrograph the spectrum is convoluted with the image position in the large entrance slot and a unique deconvolution of the spectrum is not possible. Objects which are very much larger than the 11′ by 17′ entrance slot cause all spectral information to be lost but instead the spatial distribution of surface brightness may be measured for the bandwidths of the three channels, namely 1350–1760 Å, 1760–2160 Å, and 2150–2550 Å. When viewing extended objects these are effectively broad band photometers with the same passbands and are therefore similar to the photometric channel except that its slot is 1.7′ by 17′. There are thus four broad band photometric measurements of surface brightness, at wavelengths centred near 1550, 1950, 2350 and 2740 Å.

From the known spectral sensitivities of each detector channel it is possible to calculate the relation between the surface brightness $S(\lambda)$ in J cm^{-2} s^{-1} Å^{-1} deg^{-2} and the number of photons, N, registered in the integration interval of 0.148 s. These are: $S(1550\ \text{Å}) = 5.77\times10^{-19}\ N$, $S(1950\ \text{Å}) = 5.47\times10^{-19}\ N$, $S(2350\ \text{Å}) = 4.61\times10^{-19}\ N$, $S(2740\ \text{Å}) = 2.66\times10^{-19}\ N$.

The Royal Society is collaborating with JSTOR to digitize, preserve, and extend access to
Philosophical Transactions of the Royal Society of London. Series A, Mathematical and Physical Sciences.
www.jstor.org

Downloaded from rsta.royalsocietypublishing.org

PHILOSOPHICAL TRANSACTIONS OF THE ROYAL SOCIETY A MATHEMATICAL, PHYSICAL & ENGINEERING SCIENCES

The pattern of sky survey

The orbit and attitude stabilization of the TD-1A spacecraft are such that the pattern of sky survey is along lines of nearly constant ecliptic longitude, the longitude increasing by about 4′ per orbit. Objects near the ecliptic poles are thus scanned very many times and the Large Magellanic Cloud (L.M.C.), with a diameter possibly as large as 10° (de Vaucouleurs 1954, 1960) and only a few degrees from the south ecliptic pole is scanned about 1000 times, each time along a slightly different path. The Small Magellanic Cloud (S.M.C.) is about 25° from the south ecliptic pole and is scanned about 120 times.

The paths of two typical scans through the L.M.C. are superimposed on an Uppsala–Mt Stromlo yellow light print in figure 1, plate 17. They are seen to diverge from the south ecliptic pole at $\alpha = 6$ h 00, $\delta = -66° 33'$. The separation of the parallel lines corresponds to the 17′ projected width of the focal plane slots.

Observations

Single scans

As a consequence of the large number of overlapping scans of the L.M.C. and S.M.C., the most accurate measurements are obtained by averaging adjacent scans, making allowance for the slightly different path of the slit across the sky. Nevertheless, both L.M.C. and S.M.C. are sufficiently bright to be detected in a single scan and the signals detected from the L.M.C. on orbits 680 and 854 are shown in figures 6 and 7 respectively. On orbit 680 the 30 Dor complex is seen between $\lambda = -87°$ and $\lambda = -86°$ while on orbit 854 there are two bright regions, a region to the south of NGC 2009, at $\lambda = -86°$ and the bar of the L.M.C. at $\lambda = -85°$. Figure 1 shows the paths scanned on these two orbits and also the regions referred to above.

Maps of surface brightness

A convenient way of displaying the large amount of data available for the L.M.C. is in the form of simulated photographs. The individual orbital scans are transformed into equatorial coordinates in a grid of 128 × 128 elements. Each element of the grid represents an area 2.8′ by 2.8′ and is the mean of about 16 orbital scans. The intensity corresponding to each grid element is plotted as a grey scale on an SC4020 graph plotter. This procedure is repeated for each of the four passbands and the results are displayed in figures 2–5, plate 18. The darker areas correspond to high surface brightness as in a conventional photographic plate and the gaps in the coverage arise because the data reduction is not yet complete. The rectangle in the top left of each map shows the projected size of the appropriate scanning aperture.

A comparison of the u.v. data with the yellow light plates of the Uppsala–Mt Stromlo survey of the Magellanic Clouds shows that the prominent u.v. features are easily identifiable with visible features as set out in table 1.

Photometric results

As an example of the photometric measurements available, the spectral distribution of u.v. flux from four regions, two in the L.M.C. and two in the S.M.C., are shown in figures 8–10.

The measured fluxes from the 'bar' of the L.M.C. are shown in figure 8. As a comparison the u.v. flux distribution from unreddened stars distributed according to a luminosity function

Downloaded from rsta.royalsocietypublishing.org

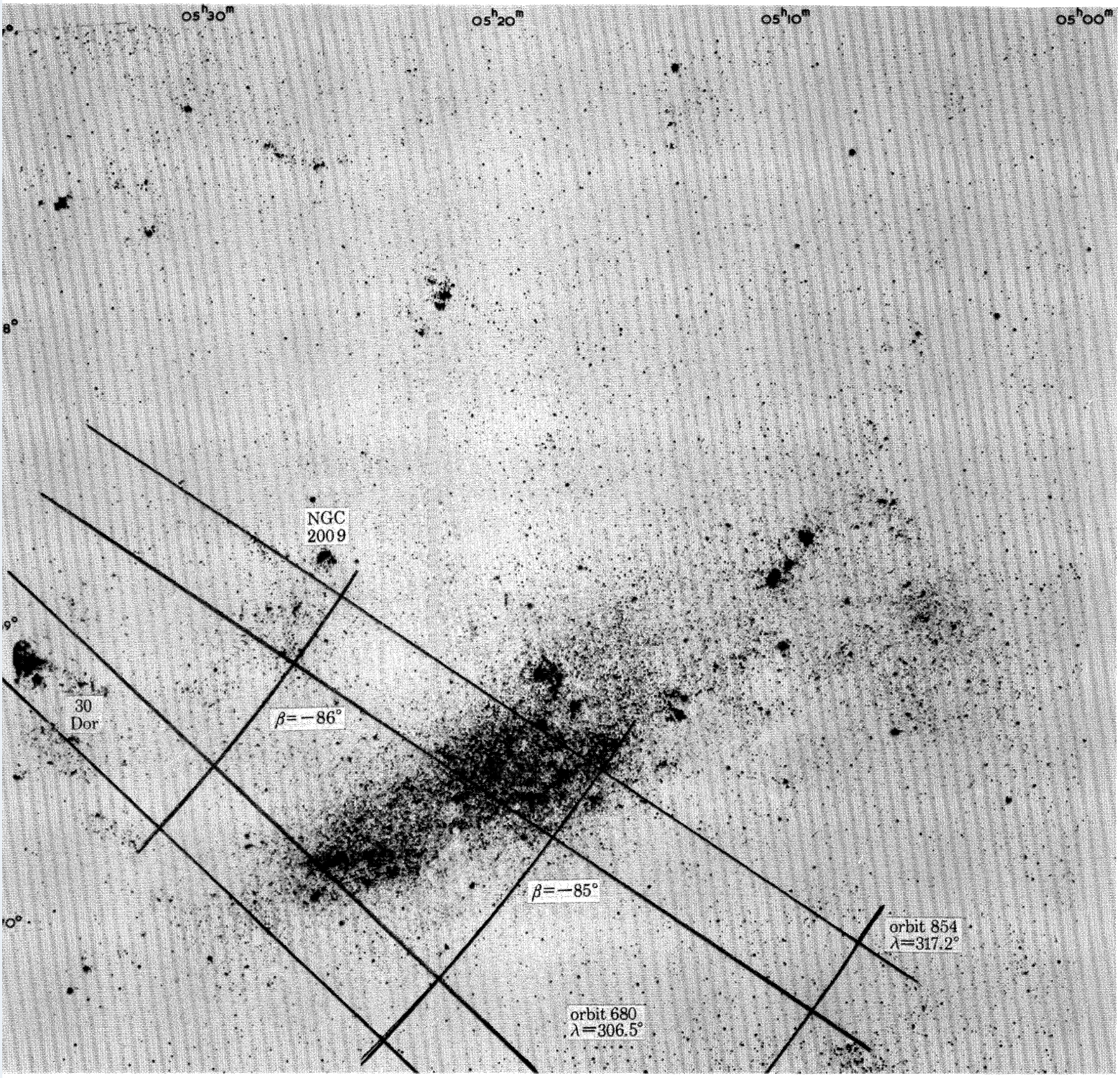

FIGURE 1. Uppsala–Mt Stromlo print of the Large Magellanic Cloud taken in yellow light. The ultraviolet scan paths of TD-1 are shown for orbits 680 and 854.

(*Facing p.* 474)

PHILOSOPHICAL TRANSACTIONS OF THE ROYAL SOCIETY A MATHEMATICAL, PHYSICAL & ENGINEERING SCIENCES

PHILOSOPHICAL TRANSACTIONS OF THE ROYAL SOCIETY A MATHEMATICAL, PHYSICAL & ENGINEERING SCIENCES

Downloaded from rsta.royalsocietypublishing.org

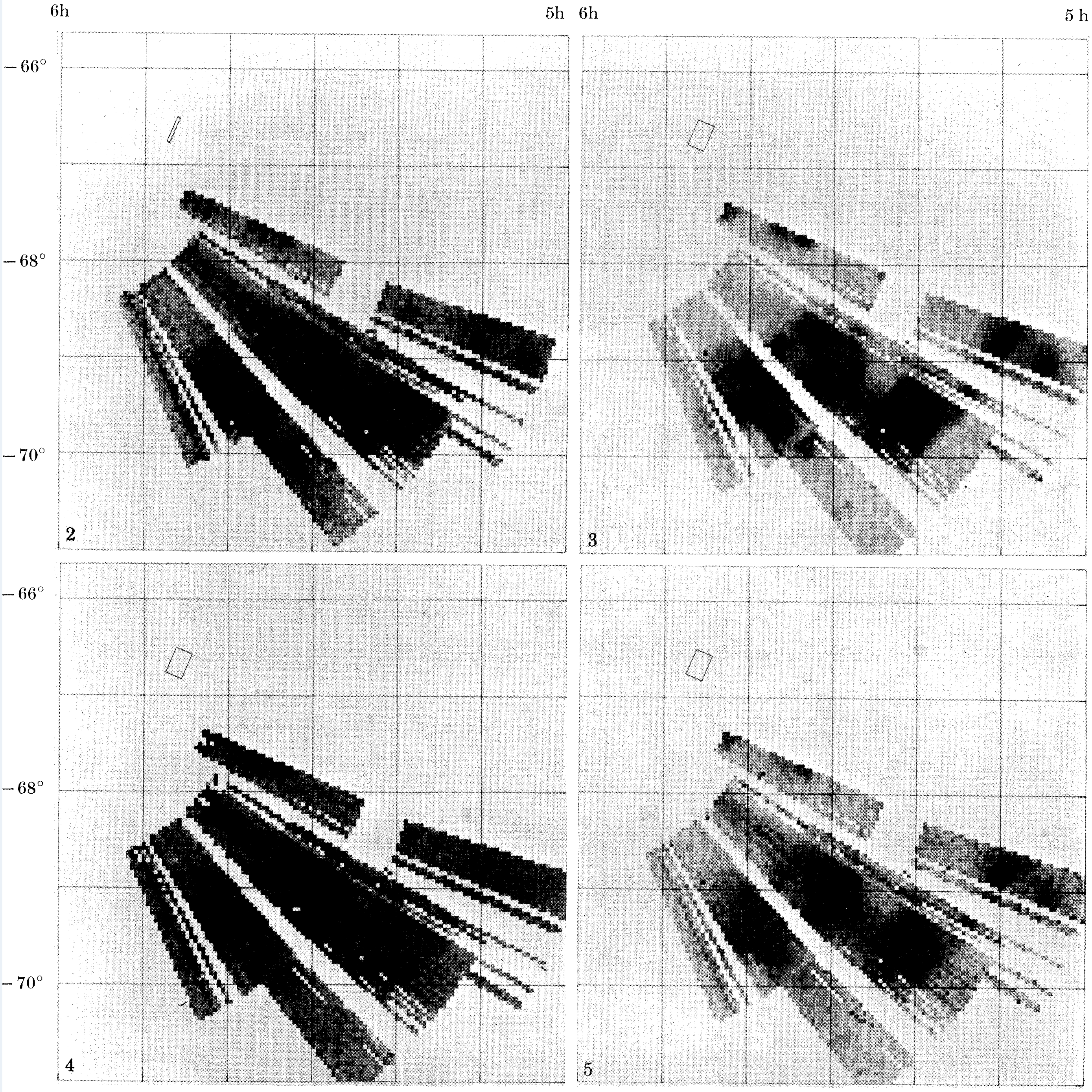

Figure 2. Ultraviolet map of Large Magellanic Cloud. Channel A1, 2740 Å.
Figure 3. Ultraviolet map of Large Magellanic Cloud. Channel A2, 1550 Å.
Figure 4. Ultraviolet map of Large Magellanic Cloud. Channel A3, 1950 Å.
Figure 5. Ultraviolet map of Large Magellanic Cloud. Channel A4, 2350 Å.

PHILOSOPHICAL TRANSACTIONS OF THE ROYAL SOCIETY A MATHEMATICAL, PHYSICAL & ENGINEERING SCIENCES

Downloaded from rsta.royalsocietypublishing.org

TABLE 1. PROMINENT FEATURES IN THE LARGE MAGELLANIC CLOUD

coordinates α	coordinates δ	visible feature	comments
5 h 05 min	69° 00′	‘spiral arm’ from NW end of bar	neutral colour in visible
5 h 10 min	68° 50′	extension of ‘bar’ to NW; includes NGC 1850, 1858	blue in visible (1)
5 h 14 min	69° 25′	NGC 1972, 1874, 1876, 1877, 1880	blue in visible (1)
5 h 20 min	69° 30′	bar of L.M.C.	N–S extent apparently greater in far u.v. than in visible
5 h 30 min	69° 00′	region of blue stars SE of NGC 2009; includes NGC 2060, 2069, 2070	relatively more prominent in u.v. than in visible light
5 h 33 min	69° 54′	region of blue stars	—
5 h 38 min	69° 25′	region of blue stars	—
5 h 40 min	68° 05′	30 Dor	extensive region of emission nebulosity; very blue in visible (1)
5 h 42 min	69° 30′	emission nebulosity N 159 (2)	—

References: (1) Walker, Blanco & Kunkel (1969), (2) Henize (1956).

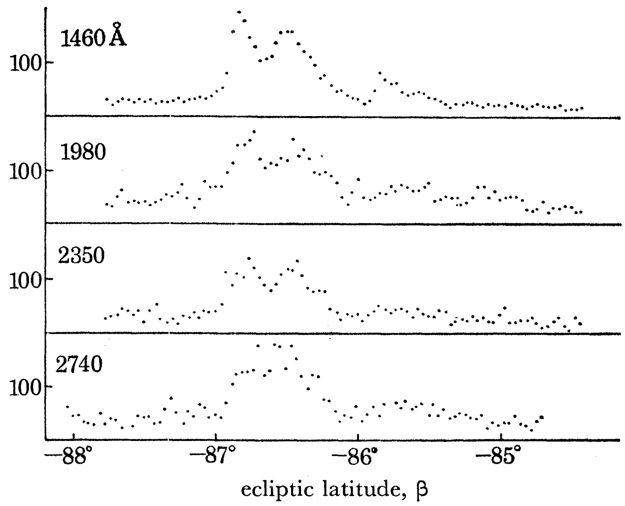

FIGURE 6. Scan through Large Magellanic Cloud on orbit 680 (see figure 1), $\lambda = 306.5°$.

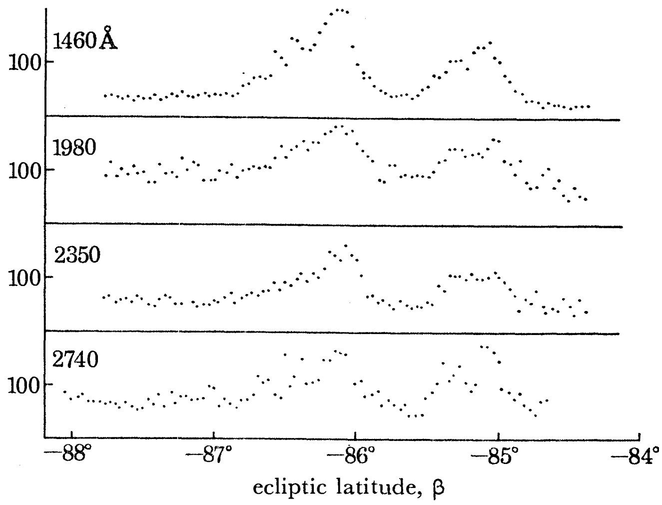

FIGURE 7. Scan through Large Magellanic Cloud on orbit 854 (see figure 1), $\lambda = 317.2°$.

Downloaded from rsta.royalsocietypublishing.org

appropriate to our own galaxy (Gondhalekar & Wilson 1974) is shown, but normalized to agree with the measured L.M.C. flux at 2740 Å. The difference between the measured fluxes and the comparison curve is most easily explained as due to reddening but the alternative explanation of a different stellar luminosity function for the L.M.C. compared with the Galaxy cannot be ruled out.

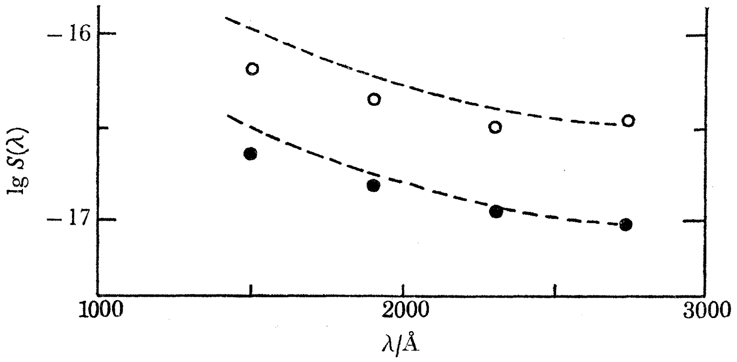

FIGURE 8. Measured ultraviolet fluxes of (○) the L.M.C.-bar and (●) the S.M.C.-bar compared with a flux distribution expected from unreddened stars with a galactic luminosity function normalized to the 2740 Å measurement in each case.

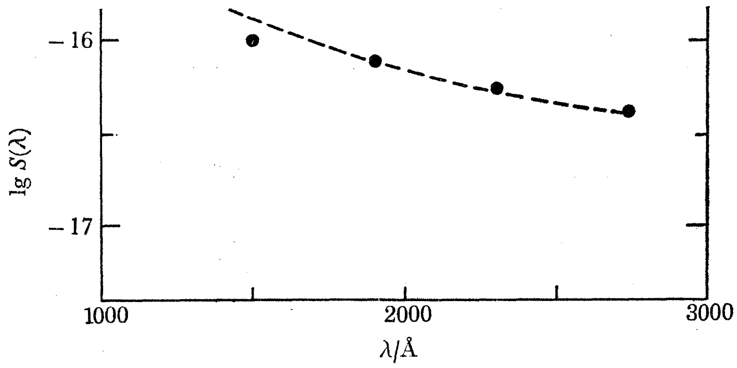

FIGURE 9. Measured ultraviolet fluxes from the H II region 30 Doradus in the L.M.C. compared with that expected from unreddened stars with a galactic luminosity function normalized to the 2740 Å measurement.

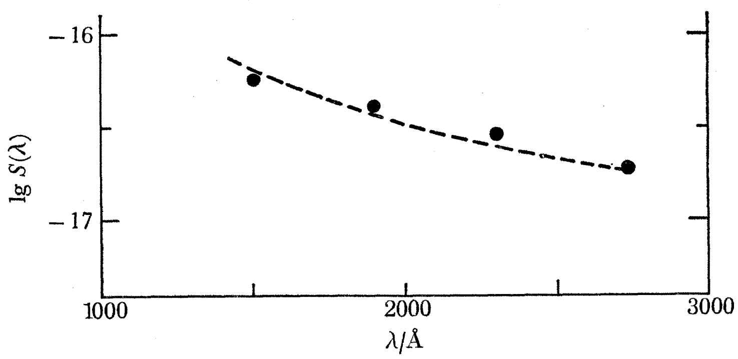

FIGURE 10. Measured ultraviolet fluxes from the H II region NGC 346 in the S.M.C. compared with that expected from unreddened stars with a galactic luminosity function normalized to the 2740 Å measurement.

PHILOSOPHICAL TRANSACTIONS OF THE ROYAL SOCIETY A MATHEMATICAL, PHYSICAL & ENGINEERING SCIENCES
PHILOSOPHICAL TRANSACTIONS OF THE ROYAL SOCIETY A MATHEMATICAL, PHYSICAL & ENGINEERING SCIENCES

Downloaded from rsta.royalsocietypublishing.org

Figure 8 also shows the u.v. fluxes measured from the 'bar' of the S.M.C. These fluxes are of a preliminary nature since little data have yet been accumulated for the S.M.C. and the statistical uncertainty in the measurements is larger than will eventually be the case when the full data have been reduced. The comparison with unreddened galactic stars, again normalized to the 2740 Å measurement, is also included.

Clearly the S.M.C. has a substantially lower ultraviolet surface brightness than the L.M.C., by a factor of about three. The observational errors are such that no significant difference in u.v. colours between L.M.C. and S.M.C. are detectable although it appears that the S.M.C. has a slightly higher ultraviolet gradient than the L.M.C. The smaller surface brightness of the S.M.C. is probably due to a smaller space density of early type stars.

The emission nebulae in the Magellanic Clouds have been studied by Henize (1956) and he notes that the space density of emission nebulae in the S.M.C. is similar to that in the L.M.C. but the S.M.C. nebulae are of lower brightness. This is interpreted as due to a lower density of the interstellar medium in the S.M.C., which if true would give rise to a smaller space density of early type stars and would be in accord with the observed lower surface brightness of the S.M.C. compared with the L.M.C.

Figures 9 and 10 show the u.v. fluxes from two prominent H II regions – 30 Doradus (the giant region of nebulosity in the L.M.C.) and NGC 346 in the S.M.C. In each case the flux distribution is significantly more ultraviolet than in the bar region of the corresponding cloud as would be expected qualitatively to allow for the very hot stars necessary to produce the H II nebulosities. The comparison curves are the same as before and show that the observed colours are in reasonable agreement with those expected from unreddened stars with a galactic luminosity function. It is a little surprising that the exciting stars, whose flux distributions would be much more ultraviolet than that observed, do not make a greater contribution to the curve. A possible solution is interstellar extinction but this would have to be different from that observed in our own galaxy (Bless & Savage 1970; Nandy *et al.* 1974) in that there is no evidence of the extinction maximum near 2200 Å. It is more likely that the solution lies in the luminosity function and that a significant contribution to the ultraviolet flux is made by stars other than those exciting the nebulae.

We would like to thank Dr G. I. Thompson of the Royal Observatory, Edinburgh, and staff of the Atlas Computer Laboratory, Chilton, for making available the S2-86 data.

References (Evans *et al.*)

Bless, R. C. & Savage, B. D. 1970 Ultraviolet stellar spectra and related ground based observations. *I.A.U. Symposium* (ed. L. Houziaux & H. E. Butler), no. 36, p. 28.

Boksenberg, A., Evans, R. G., Fowler, R. G., Gardner, I. S. K., Houziaux, L., Humphries, C. M., Jamar, C., Macau, D., Macau, J. P., Malaise, D., Monfils, A., Nandy, K., Thompson, G. I., Wilson, R. & Wroe, H. 1973 *Mon. Not. R. astr. Soc.* **163**, 291.

Gondhalekar, P. M. & Wilson, R. 1974 *Astron. & Astrophys.* (To be published.)

Henize, K. G. 1956 *Astrophys. J. Suppl.* **2**, 315.

Nandy, K., Thompson, G. I., Jamar, C., Monfils, A. & Wilson, R. 1974 *Phil. Trans. R. Soc. Lond.* A **279**, 337. (this volume).

de Vaucouleurs, G. 1954 *Observatory* **74**, 158.

de Vaucouleurs, G. 1960 *Astrophys. J.* **131**, 265.

Walker, M. F., Blanco, V. M. & Kunkel, W. E. 1969 *Astron. J.* **74**, 44.

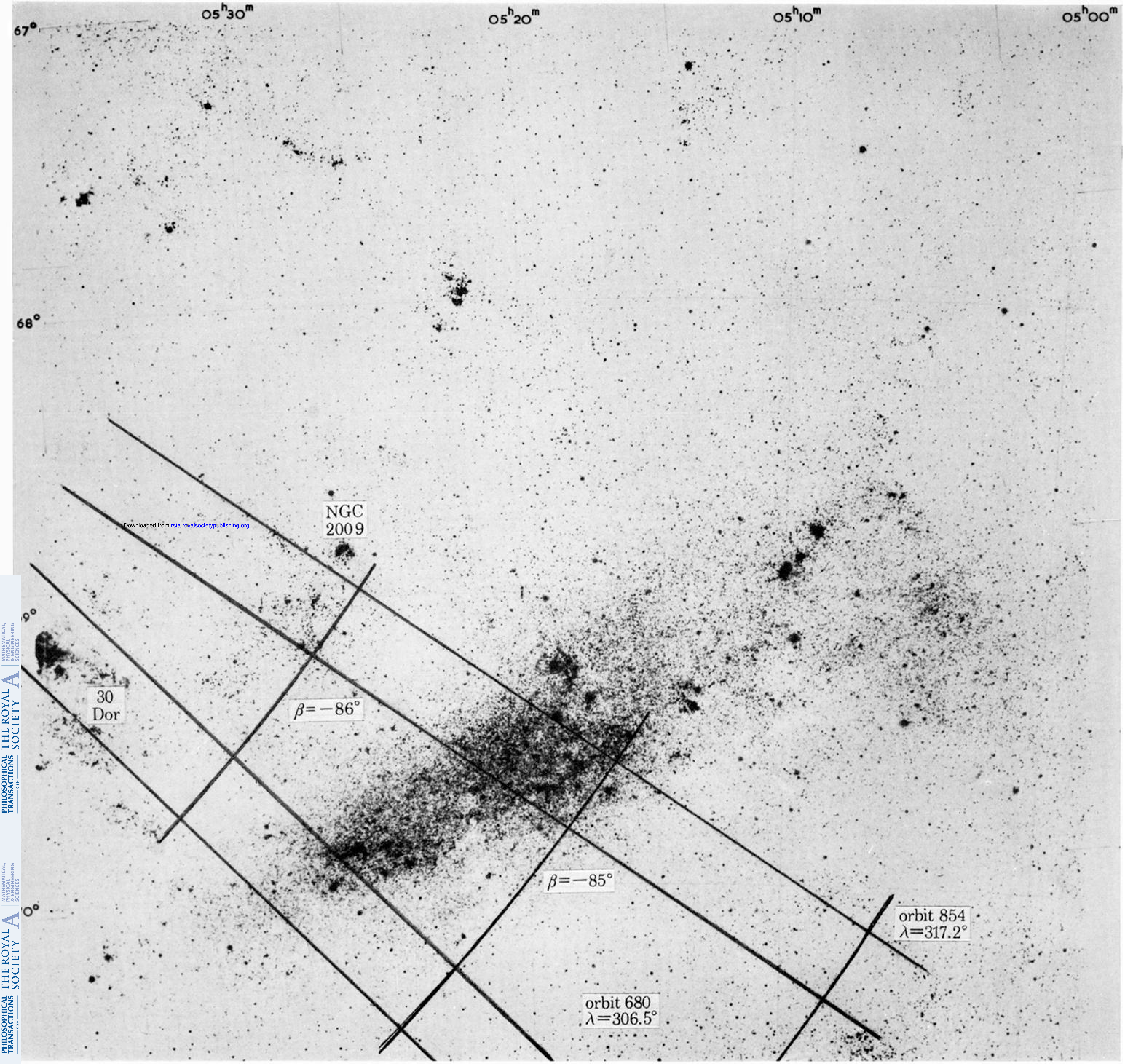

FIGURE 1. Uppsala–Mt Stromlo print of the Large Magellanic Cloud taken in yellow light. The ultraviolet scan paths of TD-1 are shown for orbits 680 and 854.

Downloaded from rsta.royalsocietypublishing.org

PHILOSOPHICAL TRANSACTIONS OF THE ROYAL SOCIETY A MATHEMATICAL, PHYSICAL & ENGINEERING SCIENCES

PHILOSOPHICAL TRANSACTIONS OF THE ROYAL SOCIETY A MATHEMATICAL, PHYSICAL & ENGINEERING SCIENCES

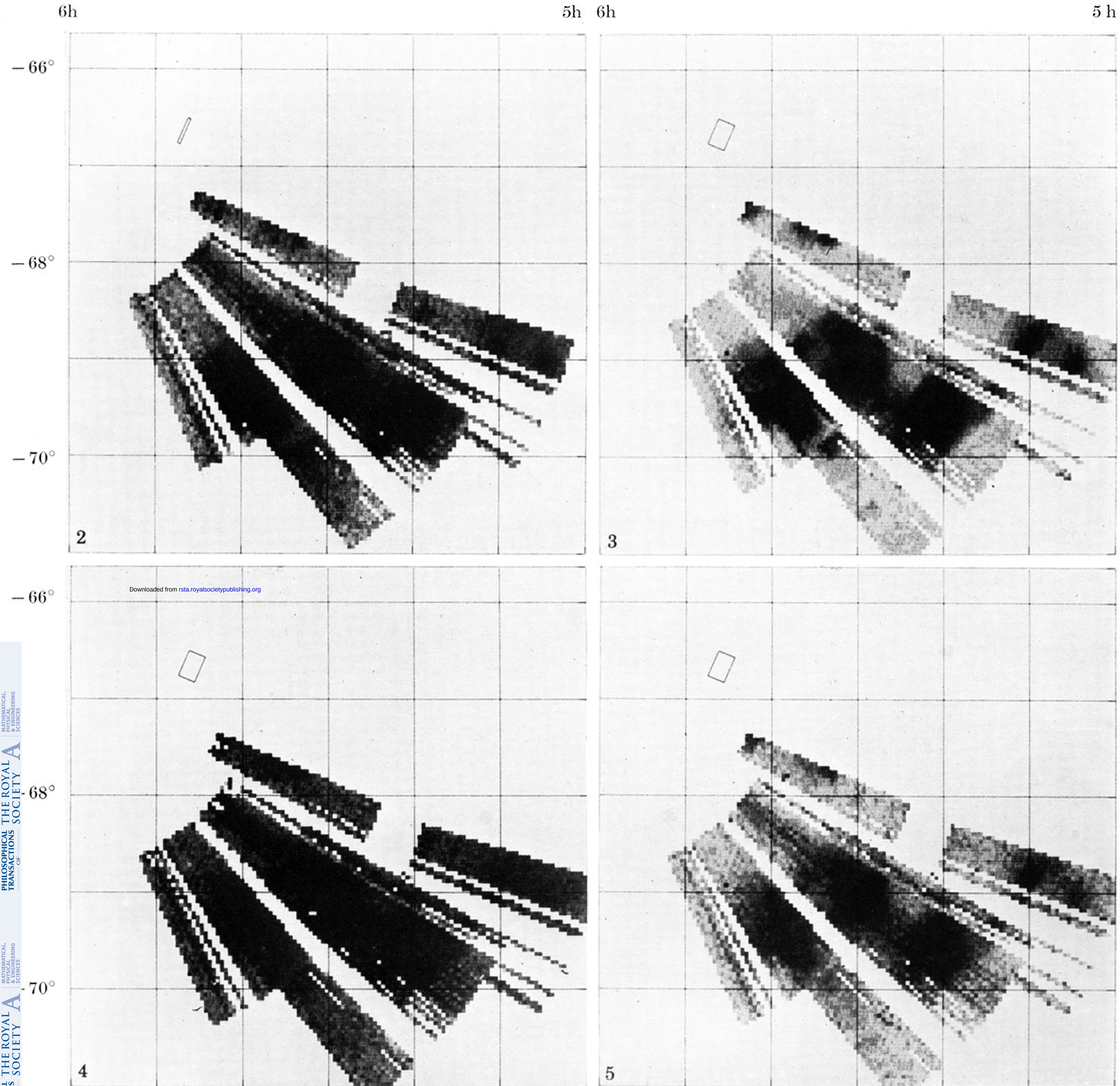

Downloaded from rsta.royalsocietypublishing.org

FIGURE 2. Ultraviolet map of Large Magellanic Cloud. Channel A1, 2740 Å.
FIGURE 3. Ultraviolet map of Large Magellanic Cloud. Channel A2, 1550 Å.
FIGURE 4. Ultraviolet map of Large Magellanic Cloud. Channel A3, 1950 Å.
FIGURE 5. Ultraviolet map of Large Magellanic Cloud. Channel A4, 2350 Å.